

Received: 3 October 2020

Revised: 16 November 2020

Accepted: 17 November 2020

DOI: 10.1002/jcc.26458

**FULL PAPER**Journal of  
**COMPUTATIONAL**  
**CHEMISTRY** WILEY

# Electronic couplings for singlet fission: Orbital choice and extrapolation to the complete basis set limit

Tom Speelman<sup>1</sup>  | Ana V. Cunha<sup>2</sup> | R. K. Kathir<sup>3</sup> | Remco W. A. Havenith<sup>1,3,4</sup> <sup>1</sup>Stratingh Institute for Chemistry, University of Groningen, Groningen, The Netherlands<sup>2</sup>High Performance Computing Group, SURFSara, Amsterdam, The Netherlands<sup>3</sup>Zernike Institute for Advanced Materials, University of Groningen, Groningen, The Netherlands<sup>4</sup>Department of Inorganic and Physical Chemistry, Ghent University, Ghent, Belgium**Correspondence**

Ana V. Cunha, SURFSara, Science Park 140, 1098 XG Amsterdam, The Netherlands. Email: ana.dacunha@surf.nl

**Funding information**

Nederlandse Organisatie voor Wetenschappelijk Onderzoek, Grant/Award Number: 15CSER73; U.S. Department of Energy, Grant/Award Number: DE-AC05-00OR22725

**Abstract**

For the search for promising singlet fission candidates, the calculation of the effective electronic coupling, which is required to estimate the singlet fission rate between the initially excited state ( $S_0S_1$ ) and the multiexcitonic state ( $^1TT$ , two triplets on neighboring molecules, coupled into a singlet), should be sufficiently reliable and fast enough to explore the configuration space. We propose here to modify the calculation of the effective electronic coupling using a nonorthogonal configuration interaction approach by: (a) using only one set of orbitals, optimized for the triplet state of the molecules, to describe all molecular electronic states, and (b) only taking the leading configurations into consideration. Furthermore, we also studied the basis set convergence of the electronic coupling, and we found, by comparison to the complete basis set limit obtained using the cc-pVnZ series of basis sets, that both the aug-cc-pVDZ and 6-311++G\*\* basis sets are a good compromise between accuracy and computational feasibility. The proposed approach enables future work on larger clusters of molecules than dimers.

**KEYWORDS**

basis set limit, effective electronic coupling, nonorthogonal configuration interaction, singlet fission

## 1 | INTRODUCTION

Singlet fission, the process in which four charge carriers can be generated by one photon, is a promising way to go beyond the Shockley-Queisser limit.<sup>1</sup> In this process, the energy of a photoexcited singlet state (usually  $S_1$ ) is partially transferred to a neighboring molecule, and both molecules end in their lowest triplet state ( $^1TT$  state); both triplet states are coupled in an overall singlet. This process is spin allowed, and can therefore be a very fast process.<sup>2-7</sup>

Singlet fission has been observed in amongst others tetracene and numerous studies have been devoted to unravel the singlet fission mechanism in tetracene, and tetracene derivatives (see for example <sup>8-19</sup>). Even though it has been found that singlet fission in

tetracene is temperature independent,<sup>20</sup> in this case, singlet fission is slightly endoergic, occurring at a 40 ps timescale.<sup>21</sup>

To describe the singlet fission process, one can work in the adiabatic or in the diabatic representation (see for a detailed discussion Ref. <sup>4</sup> and references cited). In the adiabatic representation, the first and second derivative couplings govern the mixing between the adiabatic electronic potential energy surfaces; the transition between states is determined by nuclei displacements, that is, nonadiabatic couplings. A simple approach to estimate the nonadiabatic couplings was developed by Krylov et al. based on the reduced one-particle transition density matrix between initial and final adiabatic states.<sup>22</sup> This method has been applied to study model singlet fission systems.<sup>23</sup> In the diabatic representation, the derivative couplings vanish

This is an open access article under the terms of the Creative Commons Attribution-NonCommercial-NoDerivs License, which permits use and distribution in any medium, provided the original work is properly cited, the use is non-commercial and no modifications or adaptations are made.

© 2020 The Authors. *Journal of Computational Chemistry* published by Wiley Periodicals LLC.

and the diabatic states are coupled through the electronic Hamiltonian. The off-diagonal matrix elements of the electronic Hamiltonian are called the electronic couplings. An approximation for the singlet fission probability, using Fermi's golden rule, is then<sup>6</sup>

$$w(SF) = h^{-1} |\langle T1T | H | S_0S_1 \rangle|^2 \rho[E] \quad (1)$$

with  $\langle T1T | H | S_0S_1 \rangle$  the effective electronic coupling between the initially excited state  $S_0S_1$  and the multiexcitonic  $T1T$  state, and  $\rho[E]$  the density of states. Note that different studies have been devoted to calculate the singlet fission dynamics (see for example<sup>24–27</sup>). The numerous methods used to estimate effective electronic couplings have different levels of complexity.<sup>4,28</sup> Electronic couplings can be extracted from the splitting in orbital energies,<sup>29</sup> using a frontier molecular orbital approach,<sup>3,30</sup> ab initio Frenkel–Davydov exciton model,<sup>31–32</sup> or a rigorous nonorthogonal configuration interaction (NOCI) scheme.<sup>18,33</sup> Hence, it is crucial for singlet fission research that the procedure used for the evaluation of effective electronic couplings has not only sufficient accuracy, but is also computationally fast enough to be used for studying large molecules in many different orientations, and can still be interpreted in terms of chemical concepts.

Recently, a study in which the packing of two ethylene molecules as a model for singlet fission was optimized<sup>34</sup> has been published. Here, the electronic coupling between the  $S_0S_1$  and  $T1T$  states was evaluated for many different configurations of two ethylene molecules using an approximate model, termed as “simple” model,<sup>3,17</sup> and a comparison between the electronic couplings calculated using the “simple” model and an ab initio NOCI approach was made. It was found that both methods were able to distinguish the configurations with large and small couplings. This model system was also studied in the adiabatic representation,<sup>23</sup> and it was shown that the two different methods do not always agree: for a perfectly stacked dimer, large nonadiabatic couplings were found, whereas contrary predictions were derived based on the model Hamiltonians of Michl et al.<sup>7</sup> However, for the slip-stacked configurations, both methods were in agreement and larger values of the nonadiabatic coupling were found.

In the aforementioned NOCI approach, the wavefunction for a dimer is written as a linear combination of so-called many-electron basis functions (MEBFs), which are spin-adapted, antisymmetrized products of molecular wavefunctions.<sup>35–36</sup> Hence, in case of a dimer AB, each MEBF is a product of two molecular wavefunctions, one describing the electronic state of molecule A and one describing the electronic state of molecule B. Therefore, the MEBFs can easily be assigned to the diabatic  $S_0S_0$ ,  $S_0S_1$ ,  $S_1S_0$ , and  $T_1T_1$  ( $T1T$ ) states. Charge transfer (CT) states can be constructed as spin-adapted, antisymmetrized products of cationic and anionic wavefunctions. In prior applications of this method,<sup>19,33</sup> state-specific CASSCF wavefunctions were used to construct the MEBFs. Advantages of this approach are the inclusion of static correlation and orbital relaxation effects. However, the use of MEBFs constructed from (state-specific) CASSCF wavefunctions increases the computational complexity: if the CASSCF wavefunctions for each of the monomers consists of  $L$  Slater determinants, the MEBF consists of  $L^2$  determinants.

Moreover, the Hamiltonian matrix element  $\langle T1T | H | S_0S_1 \rangle$  is in that case written as a sum of  $L^4$  Hamiltonian matrix elements over Slater determinants  $\Delta_i$ ,  $\langle T1T | H | S_0S_1 \rangle = \sum_{i=1}^{L^2} \sum_{j=1}^{L^2} C_i C_j \langle \Delta_i | H | \Delta_j \rangle$ . For decent CASSCF wavefunctions of sufficient length, this scaling prohibitively limits the applicability of the method. Furthermore, the nonorthogonality caused by the use of different orbital sets for different electronic states increases the computational complexity for the matrix element evaluation over determinant pairs. These problems have been addressed by the introduction of a reduced common orbital basis,<sup>37</sup> which is made of the combined sets of molecular orbitals occupied in any of the determinants used to describe the states of each molecule. The linear dependencies are removed from this set according to a threshold  $\tau_{MO}$ . It was determined empirically that the threshold  $\tau_{MO}$  could be chosen to be rather large ( $\sim 10^{-3}$ ) for the electronic states of interest without loss of accuracy in the calculated couplings. This observation suggests that the calculated coupling is not very sensitive to the differences in the orbital sets for different states. In this same work, another threshold,  $\tau_{det}$ , is introduced to eliminate determinant pair combinations for which the product of CI coefficients,  $C_i C_j$  is smaller than  $\tau_{det}$ . Again, it was found that many determinant pairs could be eliminated ( $\tau_{det} \sim 10^{-4}$ ) without loss of accuracy. These results suggest that the effective coupling is dominated by only the matrix element over the leading configuration state functions of each diabatic state. The computational expense of the aforementioned NOCI approach thwarted in the past the use of large basis sets. However, as the coupling between  $T1T$  and  $S_0S_1$  is mainly determined by the overlap between the orbitals of one molecule with its neighbor, large basis sets may be required to describe the intermolecular region correctly.

The above considerations on the NOCI method for the evaluation of singlet fission couplings prompted us to study the complete basis set limit for the electronic coupling, using a simplified version of the NOCI method. We suggest to use only one set of orbitals to describe the leading configurations of the molecular  $S_0$ ,  $S_1$ ,  $T_1$ ,  $D_0^+$ ,  $D_0^-$  states, required to form the MEBFs. In this ansatz, only a single configuration is taken as the MEBF (see also for example<sup>38–39</sup>), and that only one orbital set is used to describe the various molecular electronic states, contrarily to the previous application of the NOCI method. Furthermore, considering that the  $S_1S_0/S_0S_1$  MEBFs already differ in two spin orbitals from the  $T1T$  configuration, the contributions from other determinant pairs are expected to be very small. Thus, it is expected that only a few configurations are important, and that the largest contribution is already captured when taking only the leading configurations into account. Only in the cases that the states of interest cannot be described properly by a few main configurations, sizeable effects of (static) correlation are expected.

The suitability of this simplified approach will be tested first on a tetracene dimer (Figure 1(A)) where we determine the effect of truncating the CI expansion. A second test is performed on an ethylene dimer taken from Ref.<sup>34</sup> (Geometry 1a, Figure 1(B)), where we study the effect of using various orbital sets. Note that in the case of the ethylene dimer, the previously performed CASSCF(2,2) calculations

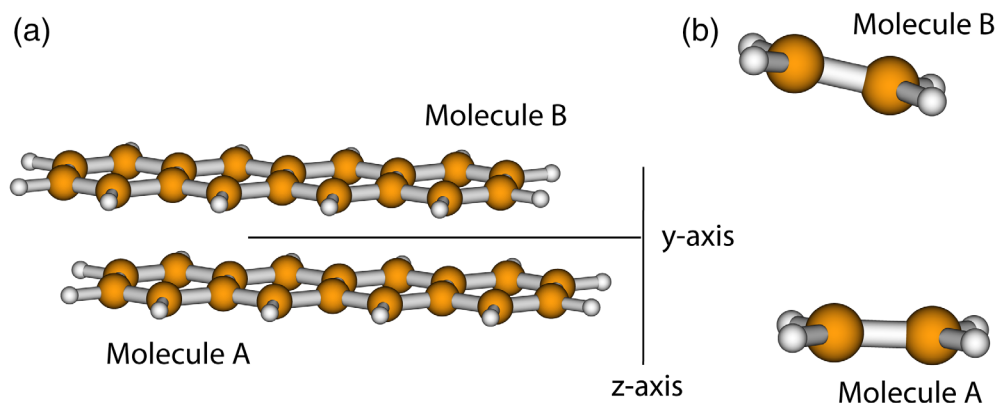


**FIGURE 1** The geometry of (A) the tetracene dimer and (B) ethylene dimer used in this study (geometry 1a of ref. <sup>34</sup>). Cartesian coordinates of these dimers are supplied in supporting information, tables S1–S2

were already one configuration wavefunctions for  $S_1$  and  $T_1$ , due to spatial and spin symmetry. As there are different possible ways to generate initial orbital sets to construct the relevant configurations, various possibilities are tested (e.g., CASSCF, HF, Kohn–Sham orbitals generated using different DFT functionals). After that, the complete basis set limit will be determined for the electronic coupling between the  $S_0S_1$  and  ${}^1TT$  states. We show that there are stringent requirements to the basis set for an accurate evaluation of this property.

## 2 | COMPUTATIONAL METHODS

For the tetracene dimer (Figure 1(A), Table S1), state specific CASSCF (6,6) and CASSCF(4,4) calculations were performed using GAMESS-UK<sup>40</sup> to obtain the wavefunctions for the  $S_0$  ( $A_g$ ),  $S_1$  ( $B_{1u}$ ), and  $T_1$  ( $B_{1u}$ ) states. The cc-pVDZ basis set,<sup>41</sup> taken from the basis set exchange library,<sup>42–44</sup> was used in all calculations. The calculations of the H/S matrix elements with state specific orbitals were performed with GronOR,<sup>35–36</sup> following the procedure outlined in Ref. <sup>37</sup> with both  $\tau_{MO}$  and  $\tau_{det}$  equal to  $10^{-5}$ . The calculations of the H/S matrix elements using one set of orbitals (natural orbitals of the unrestricted PBE calculation on the triplet state, with further canonicalization of the singly occupied orbitals) and considering only one configuration were performed with TURTLE,<sup>45</sup> the VBSCF<sup>46–47</sup> program implemented in GAMESS-UK (note that TURTLE is also able to handle multi configurational wavefunctions and different orbital sets for different electronic states). In both the GronOR and TURTLE calculations, the following four MEBFs were constructed,  $|S_0S_0\rangle$ ,  $|S_1S_0\rangle$ ,  $|S_0S_1\rangle$ , and  $|T_1T_1\rangle$ . The effective electronic coupling between two diabatic states (MEBFs) was calculated according to Equation (2).

$$t_{if}^{eff} = \frac{H_{if} - H_{av}S_{if}}{1 - S_{if}^2}; \quad H_{av} = \frac{H_{ii} + H_{ff}}{2} \quad (2)$$

In this equation,  $H_{if}$  is the Hamiltonian matrix element between the initial ( $i$ ) and final ( $f$ ) diabatic, nonorthogonal states,  $S_{if}$  their overlap, and  $H_{ii}/H_{ff}$  the energies of the initial and final states.

The calculations on the ethylene dimer were performed on Geometry 1a of Ref. <sup>34</sup> (Figure 1(B), Table S2) using GAMESS-UK.<sup>40</sup> For this geometry, prior NOCI calculations performed with GronOR<sup>35</sup> are available in Ref. <sup>34</sup>. In those calculations, the 6-311G basis set was used, and state specific CASSCF(2,2) calculations were performed to obtain the wavefunctions for the molecular  $S_0$ ,  $S_1$ ,  $T_1$ ,  $D_0^+$ , and  $D_0^-$  states. These calculations serve as a reference for determining which orbitals would be most appropriate to use to generate the configurations for the set of calculations using only one set of orbitals.

Orbitals were generated in different ways (see Text) for the closed-shell ground state and triplet state (UDFT) for each molecule. The UHF/UDFT spin free natural  $\pi_u$  and  $\pi_g^*$  orbitals were canonicalized. The orbitals for each molecule were then projected on the basis functions of the dimer (the order of the orbitals was chosen to be the occupied  $\sigma$  orbitals for each monomer first, then the  $\pi_u^A$  and  $\pi_g^{*A}$  orbitals for monomer A, followed by the  $\pi_u^B$  and  $\pi_g^{*B}$  orbitals for monomer B). In this way, all occupied  $\sigma$  orbitals of both molecules could be treated as frozen core orbitals in the subsequent NOCI calculation.

The NOCI calculations and calculation of the H/S matrix elements were performed with TURTLE.<sup>45</sup> The following six MEBFs were constructed (branching diagram spin functions were used):

1.  $|S_0S_0\rangle$ : (core) $(\pi_u^A)^2(\pi_u^B)^2$
2.  $|S_1S_0\rangle$ : (core) $(\pi_u^A)^1(\pi_g^{*A})^1(\pi_u^B)^2$
3.  $|S_0S_1\rangle$ : (core) $(\pi_u^A)^2(\pi_u^B)^1(\pi_g^{*B})^1$
4.  $|T_1T_1\rangle$ : (core) $(\pi_u^A)^1(\pi_g^{*A})^1(\pi_u^B)^1(\pi_g^{*B})^1$
5.  $|D_1^+D_1^-\rangle$ : (core) $(\pi_u^A)^1(\pi_u^B)^2(\pi_g^{*B})^1$
6.  $|D_1^-D_1^+\rangle$ : (core) $(\pi_u^A)^2(\pi_g^{*A})^1(\pi_u^B)^1$

A VBCI calculation was performed in the basis of these six MEBFs, and the effective couplings were determined according to Equation (2). The weights ( $W$ ) of the MEBFs in the final NOCI wavefunctions were determined according to the Gallup and Norbeck scheme.<sup>48</sup>

Overlaps between the  $\pi_u$  and  $\pi_g^*$  orbitals for ethene A and B, respectively, were calculated using various functionals with the ADF suite<sup>49–50</sup> using the fragment approach. The TZ2P basis set was used (no frozen core).<sup>51</sup>

For extrapolation to the complete basis set limit, we used the procedure outlined in <sup>52-53</sup>, and we fitted the electronic couplings as a function of the cardinal number of the basis set  $n$  to:

$$Y(n) = Y(\infty) + Ae^{-n/B}. \quad (3)$$

### 3 | RESULTS AND DISCUSSION

#### 3.1 | Tetracene – validation of the leading configuration approximation

In Table 1, the effective electronic couplings between the  $S_1S_0/S_0S_1$  and the  ${}^1TT$  states, according to Equation (2), are listed for the calculations using various molecular wavefunctions. The first thing that can be seen from the data in Table 1 is that all couplings are similar, in the range of 29–36 meV. The calculation with MEBFs composed of the CASSCF(6,6) molecular wavefunctions gives the largest coupling of 36.2 meV. Using the same orbital sets, but only using the leading configurations (renormalized to 1), the coupling decreases by 3–33.0 meV.

When the active space is reduced to CASSCF(4,4), the effective electronic coupling that is obtained is 30.4 meV, which is again smaller than the couplings evaluated using CASSCF(6,6). However, when the CASSCF(4,4) orbital sets are used, but only one configuration (renormalized to 1) is used, the coupling increases to 33.2 meV. Thus, it is difficult to predict whether the coupling is under or overestimated by reduction of the number of configurations taken into account for generating the MEBFs. What is clear, is that the deviation due to a one configuration approximation is rather modest, and, considering the reduction in computational time, the one configuration approximation seems to be a fair approximation.

Especially, if the geometry dependence is considered: sliding one tetracene molecule in the  $y$ -direction (Figure 1(A)) by 0.1 or  $-0.1$  bohr gives a change in the electronic coupling of  $\pm 7$  meV. This result

**TABLE 1** The effective electronic coupling ( $t$ , in meV) between  $S_1S_0$  and  ${}^1TT$ , evaluated using different molecular wavefunctions to form the MEBFs (all with the cc-pVDZ basis set) and the timing (in s) to evaluate the H/S matrix elements

Method	$ t_{S_1S_0-{}^1TT} $	Timing <sup>a</sup>
CASSCF(6,6)	36.2	235,738
CASSCF(6,6) – 1 configuration	33.0	9
CASSCF(4,4)	30.4	946
CASSCF(4,4) – 1 configuration	33.2	9
UHF – 1 configuration	29.6	< 1
UHF – 1 configuration, $\Delta y = 0.1^b$	22.6	< 1
UHF – 1 configuration, $\Delta y = -0.1^b$	36.7	< 1

<sup>a</sup>Calculations have all been performed on 1 node of our computer cluster, consisting of 2 Intel E5-2680 CPUs (28 cores in total) and 2 Nvidia Tesla K40 GPUs.

<sup>b</sup>Molecule B has been displaced in the  $y$ -direction by  $\pm 0.1$  bohr.

emphasizes that the electronic coupling can change significantly for small displacements, and that it has to be evaluated at different configurations in order to be of predictive value, as the zero-point vibrational motion of the molecules influences the coupling considerably. This reinforces the requirement that the method that is used to derive the couplings is sufficiently fast.

#### 3.2 | Ethene—the effect of orbitals and basis sets on the effective electronic coupling

In Table 2, the effective electronic couplings between the  $S_1S_0/S_0S_1$ , and the  ${}^1TT$  states, according to Equation (2), are listed for different orbital sets. In the reference calculation, different orbital sets for the different states were used,<sup>34</sup> leading to an effective coupling of around 65 meV between the  $S_1S_0/S_0S_1$  states and the  ${}^1TT$  state. Note that, even though in the reference calculation the CASSCF(2,2) method has been used, the  $S_1$ ,  $T_1$ , and ionic states are still one configuration because of spin/spatial symmetry; deviations between the reference couplings and those evaluated here are due to differences in the orbital sets.

In the following calculations, one set of orbitals for each molecule was used to describe its different electronic states. Even though choosing one set of orbitals has the disadvantage that orbital relaxation for the different states is not included anymore, however, as shown in <sup>37</sup>, the differences between the orbital sets are usually small, especially for the inactive orbitals.

A first approximation used to simplify the calculations, was using orthogonal orbitals to describe the electronic states of the dimer, which were obtained using a Hartree–Fock (HF) calculation on the dimer, followed by Pipek–Mezey localization<sup>54</sup> of the occupied and virtual  $\pi$  orbitals. The procedure then reduces to a conventional,

**TABLE 2** The effective electronic coupling ( $t$ , in meV) between  $S_1S_0/S_0S_1$  and  ${}^1TT$ , evaluated using the ground state orbitals obtained in various ways (all with the 6-311G basis set)

Method	$ t_{S_1S_0-{}^1TT} $	$ t_{S_0S_1-{}^1TT} $
CASSCF(2,2) from Ref. <sup>34</sup>	70.7	63.8
HF (localized dimer orbitals)	26.4	26.1
CASSCF (Ground state)	50.3	35.5
HF (Ground state)	91.2	82.9
BLYP (Ground state)	74.9	64.8
B3LYP (Ground state)	78.1	68.4
PBE (Ground state)	73.6	63.6
PBE0 (Ground state)	77.7	68.2
HCTH (Ground state)	71.8	62.0
HCTH407 (Ground state)	71.9	62.2
BP86 (Ground state)	74.2	64.2
B97 (Ground state)	76.9	67.3
PW91 (Ground state)	73.6	63.6
SVWN (Ground state)	75.2	65.0

orthogonal configuration interaction calculation. The effective coupling decreases then significantly to 26 meV (Table 2), showing that removing the nonorthogonality between the orbital sets of molecule A and B of the dimer decreases the orbital interactions between the two molecules. Hence, the overlap between the orbitals of the constituent molecules governs the interaction between the diabatic excited states and should not be eliminated.

The next set of orbitals that was used in the nonorthogonal configuration approach was the set consisting of the ground state orbitals obtained from a CASSCF(2,2) procedure. The use of this set of orbitals leads to too small electronic couplings as well, suggesting that these orbitals are not suitable to describe the intermolecular interaction between the diabatic excited states. These orbitals are not sufficiently diffuse to portray the  $S_1$  and/or  $T_1$  states, as they are optimized for the ground state, and the  $\pi_g^*$  orbital is optimized for recovering the electron correlation in the ground state (see Figure S1).

We continued with using ground state orbitals, now evaluated using the HF and DFT procedure using different functionals. The use of HF orbitals results in a slightly larger electronic coupling, as the LUMO is rather diffuse (Figure S1), whereas the use of DFT orbitals generated using different functionals all yields similar electronic couplings (Table 2). The couplings evaluated with all the DFT functionals are close to the reference value, which suggests that all of the DFT functionals are appropriate to generate a set of molecular orbitals for the ground state molecule that can be used to describe the molecular  $S_1$  and  $T_1$  states to form diabatic  $S_1S_0/S_0S_1$  and  ${}^1TT$  states. Note that the electronic coupling shows a weak correlation with the overlap between the  $\pi_u$  (HOMO) and  $\pi_g^*$  (LUMO) orbitals of the ethene molecules (Table S3), thus the coupling can also be estimated using these overlaps for functionals that are not (yet) available in GAMESS-UK.

These results were obtained using the 6-311G basis set, and it is important to validate whether these conclusions are still valid when the basis set is enlarged. Larger basis sets, especially more diffuse

basis sets, may be more appropriate to describe the intermolecular regions. Therefore, we studied the basis set convergence of the electronic coupling (Table 3), using orbitals generated with the PBE functional (any other functional would do as the results are rather functional independent). We note no significant differences in the coupling when adding polarization functions (6-311G\*\* basis set), but the addition of diffuse functions increases the coupling considerably, indicating the importance of diffuse functions. However, in the cc-pVnZ series, we noted an ever-increasing coupling between the  $S_0S_1/S_1S_0$  and the  ${}^1TT$  states, when using the ground state orbitals. As the  $\pi_g^*$  (LUMO) is not occupied in the ground state calculation, when the orbitals are optimized, this orbital may become too diffuse with increasing basis set size to properly describe the  $S_1$  and  $T_1$  states in which it is occupied. Therefore, we also used the triplet orbitals in the calculation of the electronic couplings. The UPBE spin-free natural orbitals, with further canonicalization of the  $\pi_u$  and  $\pi_g^*$  orbitals were used in the calculations listed in Table 3, under the heading 'Triplet state'. The use of triplet orbitals has the additional advantage that orbital relaxation effects are included in the diabatic  ${}^1TT$  state, and furthermore, the triplet orbitals are usually similar to the orbitals of the corresponding singlet excited state.

The results in Table 3 show that the use of the triplet orbitals reduces the coupling compared to the use of the ground state orbitals. The coupling also shows an increase with increasing basis set size. The smaller coupling that is obtained with the triplet state orbitals suggests that the  $\pi_g^*$  orbital in the triplet state is less diffuse than in the ground state. This is further substantiated with a plot of the electron density of the  $\pi_g^*$  orbital (Figure 2) along the z-axis (indicated in Figure 1). The plot shows that indeed the ground state LUMO is more diffuse than it is in the triplet state, and the density in the intermolecular region is higher, leading to a larger overlap between the orbitals localized on the different molecules, resulting in a higher

**TABLE 3** The effective electronic coupling ( $t$ , in meV) between  $S_1S_0/S_0S_1$  and  ${}^1TT$ , evaluated using the ground state and triplet UDFT natural/canonicalized orbitals obtained with different basis sets (all with the PBE functional)

Basis set	Ground state		Triplet state	
	$ t_{S_1S_0-{}^1TT} $	$ t_{S_0S_1-{}^1TT} $	$ t_{S_1S_0-{}^1TT} $	$ t_{S_0S_1-{}^1TT} $
6-311G	73.6	63.6	66.6	56.9
6-311G**	70.6	60.9	63.7	54.3
6-311++G**	108.9	108.6	88.6	85.8
cc-pVDZ	63.2	53.4	58.4	48.9
cc-pVTZ	89.5	80.8	77.4	69.2
cc-pVQZ	104.6	99.4	86.3	81.0
cc-PV5Z	111.9	110.8	89.7	87.1
cc-pV $\infty$ Z	121.5	133.2	92.8	95.3
aug-cc-pVDZ	102.9	102.7	84.5	81.7
aug-cc-pVTZ	101.2	100.1	84.0	81.2
aug-cc-pVQZ	103.5	102.7	85.3	82.8

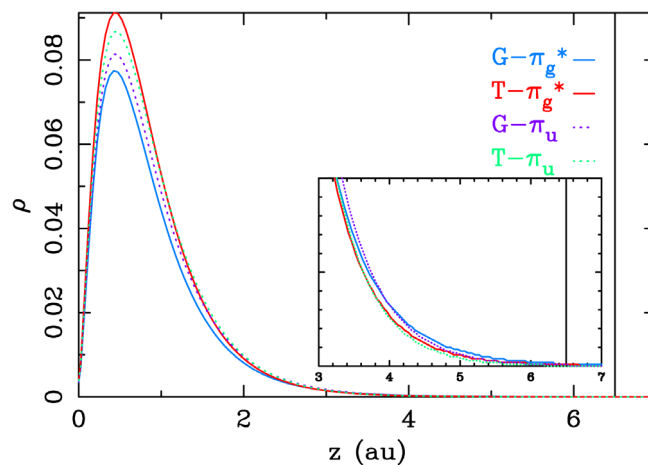


**FIGURE 2** The electron density of the  $\pi_u$  and  $\pi_g^*$  orbitals evaluated for the ground state ( $G-\pi_u/G-\pi_g^*$ ) and the triplet state ( $T-\pi_u/T-\pi_g^*$ ) of monomer a evaluated using the cc-pV5Z basis set (see also Figure 1 for indication of the z-axis). The position of the other ethene molecule is indicated with the vertical line at around  $6.5 a_0$

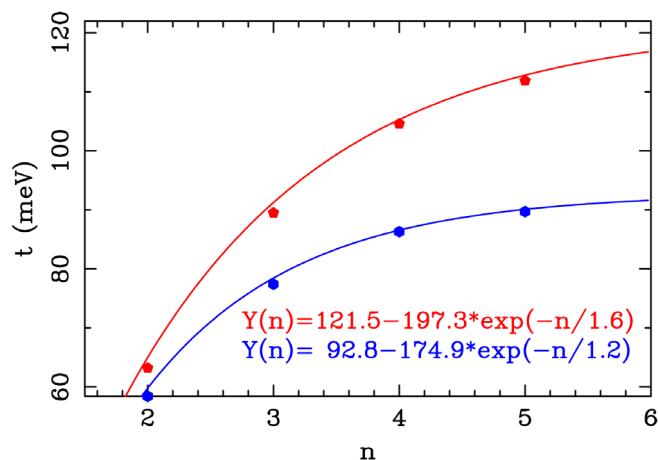


**FIGURE 3** Extrapolation to the complete basis set limit for  $|t_{S_1S_0-{}^1TT}|$  using the ground state (red) and triplet state (blue) orbitals for the cc-pVnZ basis sets

coupling. The plot further shows that the ground state  $\pi_u$  (HOMO) is also more diffuse than the triplet  $\pi_u$  orbital.

The cc-pVnZ basis sets lend themselves to extrapolate properties to the complete basis set (CBS) limit. Following the procedure outlined in <sup>52-53</sup>, we extrapolated the electronic coupling to the CBS limit according to Equation (3) (Figure 3). The CBS limit is also indicated in Table 3 as the cc-pV $\infty$ Z basis. The CBS limit for the calculations using the triplet orbitals is smaller than that obtained using the ground state orbitals. A faster convergence to the CBS limit is also achieved with the triplet orbitals. The CBS limit is considerably larger than the values obtained with the smaller 6-311G basis set, indicating that the 6-311G basis set is clearly insufficient. The use of the aug-cc-pVnZ basis sets and the 6-311++G\*\* basis set, shows that the inclusion of diffuse functions actually immediately leads to a coupling much closer to the CBS limit when the triplet state orbitals are used. The values obtained with the different aug-cc-pVnZ basis sets considered here do not differ significantly. It is important to note that there is a considerable difference between the CBS limit and the values obtained using the augmented basis sets, in the case when the ground state orbitals are used. The difference between the CBS limit and the couplings obtained using the augmented basis sets in case of the triplet orbitals is much smaller, but still in the order of 10 meV. This gives an indication of the accuracy that can be obtained. Also note that the evaluated  $S_0S_1/{}^1TT$  couplings are always smaller than the  $S_1S_0/{}^1TT$  ones, but the extrapolated value is larger. The differences obtained using the triplet orbitals are in the range of 5 meV, which falls in the error margin. From these results, we can conclude that the 6-311++G\*\* or aug-cc-pVDZ basis set is sufficient for the evaluation of electronic couplings using the triplet state orbitals.

The energies of the diabatic excited states obtained using this ansatz (Table 4) are somewhat less sensitive for the chosen basis set and orbitals. Also note that the energy does not play a large role in the evaluation of the coupling, and that the energies of the excited states can be accurately determined using other methods. Only the

**TABLE 4** The diabatic excitation energies (in eV) to the  $S_1S_0$ ,  $S_0S_1$  and  ${}^1TT$  states, evaluated using the ground state and triplet UDFT natural/canonicalized orbitals obtained with different basis sets (all with the PBE functional)

Basis set	Ground state			Triplet state		
	$S_1S_0$	$S_0S_1$	${}^1TT$	$S_1S_0$	$S_0S_1$	${}^1TT$
6-311G	10.15	10.19	6.97	10.31	10.34	6.56
6-311G**	10.03	10.06	7.10	10.11	10.14	6.61
6-311++G**	9.44	9.49	7.23	9.71	9.76	6.47
cc-pVDZ	10.13	10.16	7.09	10.19	10.22	6.64
cc-pVTZ	9.81	9.84	7.14	9.93	9.97	6.54
cc-pVQZ	9.64	9.68	7.16	9.82	9.86	6.48
cc-pV5Z	9.51	9.56	7.20	9.74	9.78	6.45
cc-pV $\infty$ Z	9.50	9.52	7.21	9.71	9.77	6.42
aug-cc-pVDZ	9.42	9.47	7.28	9.69	9.73	6.49
aug-cc-pVTZ	9.41	9.45	7.31	9.69	9.73	6.47
aug-cc-pVQZ	9.41	9.46	7.29	9.69	9.73	6.46

**TABLE 5** The final NOCI wavefunctions (cc-pV5Z basis set) and their energies of the adiabatic states in terms of the MEBFs. Gallup-Norbeck<sup>48</sup> weights (W) are reported

	$S_0$	$S_1$	$S_2$	${}^1TT$
E (eV)	0.00	9.01	10.15	6.42
MEBF	W	W	W	W
$S_0S_0$	0.998	0.006	0.000	0.001
$S_1S_0$	0.000	0.403	0.490	0.001
$S_0S_1$	0.000	0.374	0.505	0.001
${}^1TT$	0.000	0.023	0.000	0.986
$D_0^+D_0^- + D_0^-D_0^+$	0.001	0.194	0.005	0.011

energy of the  ${}^1TT$  state is significantly lower when the triplet state orbitals are used instead of the ground state orbitals. This lowering is caused by stabilization of the triplet states by using state-specific orbitals for this state, while the ground state is destabilized by this choice of orbitals, leading to a significant energy lowering of the  ${}^1TT$  state with respect to  $S_0S_0$ . Note, however, that the  $S_0S_0$  state is not involved in the calculation of the electronic coupling between  $S_1S_0/S_0S_1$  and  ${}^1TT$ , thus the use of state-specific orbitals for the ground state may improve the excitation energies, but leaves the electronic coupling unchanged.

The final NOCI wavefunctions (cc-pV5Z basis set) in terms of the MEBFs are listed in Table 5. Both the ground as the  ${}^1TT$  state are dominated by one MEBF; in the  ${}^1TT$  state, a small mixing of the charge transfer states is discernible. The  $S_1S_0$  and  $S_0S_1$  MEBFs, however, heavily mix in the final states; not only with each other, but also with the charge transfer states. As has been observed earlier,<sup>3,6-7,18-19,33</sup> this mixing with the charge transfer states enhances the coupling between the diabatic  $S_1S_0$  and  $S_0S_1$  states and

the  $^1\text{TT}$  state. To estimate the effect of the charge transfer states, we performed three separate  $3\times 3$  NOCI calculations to form new MEBFs consisting of the  $S_1S_0$ ,  $S_0S_1$ , and  $^1\text{TT}$  MEBFs mixed with the charge transfer states (Table S4), and transformed the Hamiltonian and overlap matrices to this new basis for evaluation of the coupling using Equation (2). Also, in this case, an enhanced electronic coupling of  $\sim 250$  meV is obtained.

## 4 | CONCLUSIONS

In this contribution, we have shown that the nonorthogonal configuration interaction approach to calculate the effective electronic coupling, required to estimate the singlet fission rate, between the initially excited  $S_0S_1/S_1S_0$  and the multiexcitonic  $^1\text{TT}$  states can be simplified by (a) using one orbital set to describe the different molecular electronic states, and (b) only considering the leading configurations of the diabatic states of interests. The use of an orbital set optimized for the triplet state is recommended. Moreover, we have seen from extrapolation to the complete basis set limit, that the basis set used in these calculations should be of sufficient quality and in our test case, the aug-cc-pVDZ and 6-311++G\*\* basis sets gave sufficiently accurate results, while still being computationally feasible. With these simplifications and considerations, we have proposed a method for the calculation of singlet fission couplings that is computationally fast enough, while retaining the chemical interpretability and reliability. The method is thus suitable for the exploration of different orientations of molecules in dimers, trimers, and larger clusters in the search for the most promising singlet fission candidate.

### ACKNOWLEDGMENT

RWAH acknowledges A. Varbanescu (University of Amsterdam) for enabling a GPU accelerated version of TURTLE, which will be ready for the next generation of accelerators. This work is part of the research program "Computational sciences for energy research" (project 15CSER73), which is financed by the Dutch Research Council (NWO). This research used resources (SummitDev) of the Oak Ridge Leadership Computing Facility at the Oak Ridge National Laboratory, which is supported by the Office of Science of the U.S. Department of Energy under Contract No. DE-AC05-00OR22725 (DD and ESP). This work was sponsored by NWO Exact and Natural Sciences for the use of supercomputer facilities.

### DATA AVAILABILITY STATEMENT

The data that support the findings of this study are available from the corresponding author upon reasonable request.

### ORCID

Tom Speelman  <https://orcid.org/0000-0003-2815-5381>

Remco W. A. Havenith  <https://orcid.org/0000-0003-0038-6030>

### REFERENCES

- [1] W. Shockley, H. J. Queisser, *J. Appl. Phys.* **1961**, *32*, 510.
- [2] T. C. Berkelbach, *Adv. Chem. Phys.* **2017**, *162*, 1.
- [3] E. A. Buchanan, Z. Havlas, J. Michl, *Adv. Quantum Chem.* **2017**, *75*, 175.
- [4] D. Casanova, *Chem. Rev.* **2018**, *118*, 7164.
- [5] K. Miyata, F. S. Conrad-Burton, F. L. Geyer, X.-Y. Zhu, *Chem. Rev.* **2019**, *119*, 4261.
- [6] M. B. Smith, J. Michl, *Chem. Rev.* **2010**, *110*, 6891.
- [7] M. B. Smith, J. Michl, *Annu. Rev. Phys. Chem.* **2013**, *64*, 361.
- [8] D. Casanova, *J. Chem. Theory Comput.* **2013**, *10*, 324.
- [9] A. F. Morrison, J. M. Herbert, *J. Phys. Chem. Lett.* **2017**, *8*, 1442.
- [10] P. M. Zimmerman, F. Bell, D. Casanova, M. Head-Gordon, *J. Am. Chem. Soc.* **2011**, *133*, 19944.
- [11] P. J. Vallett, J. L. Snyder, N. H. Damrauer, *J. Phys. Chem. A* **2013**, *117*, 10824.
- [12] J. J. Burdett, C. J. Bardeen, *Acc. Chem. Res.* **2013**, *46*, 1312.
- [13] G. B. Piland, C. J. Bardeen, *J. Phys. Chem. Lett.* **2015**, *6*, 1841.
- [14] X. Feng, A. I. Krylov, *Phys. Chem. Chem. Phys.* **2016**, *18*, 7751.
- [15] E. M. Grumstrup, J. C. Johnson, N. H. Damrauer, *Phys. Rev. Lett.* **2010**, *105*, 257403.
- [16] C. Quarti, D. Fazzi, M. Del Zoppo, *Phys. Chem. Chem. Phys.* **2011**, *13*, 18615.
- [17] E. A. Buchanan, Z. Havlas, J. Michl, *Bull. Chem. Soc. Jpn.* **2019**, *92*, 1960.
- [18] R. W. A. Havenith, H. D. de Gier, R. Broer, *Mol. Phys.* **2012**, *110* (19–20), 2445.
- [19] L. E. Aguilar Suarez, R. K. Kathir, E. Siagri, R. W. A. Havenith, S. Faraji, *Adv. Quantum Chem.* **2019**, *79*, 263.
- [20] M. W. B. Wilson, A. Rao, K. Johnson, S. Gélinas, R. di Pietro, J. Clark, R. H. Friend, *J. Am. Chem. Soc.* **2013**, *135*, 16680.
- [21] Z. Birech, M. Schwoerer, T. Schmeiler, J. Pflaum, *J. Chem. Phys.* **2014**, *140*, 114501.
- [22] X. Feng, A. V. Luzanov, A. I. Krylov, *J. Phys. Chem. Lett.* **2013**, *4*, 3845.
- [23] S. Matsika, X. Feng, A. V. Luzanov, A. I. Krylov, *J. Phys. Chem. A* **2014**, *118*, 11943.
- [24] A. B. Kolomeisky, X. Feng, A. I. Krylov, *J. Phys. Chem. C* **2014**, *118*, 5188.
- [25] W.-L. Chan, M. Ligges, X.-Y. Zhu, *Nat. Chem.* **2012**, *4*, 840.
- [26] T. C. Berkelbach, M. S. Hybertsen, D. R. Reichman, *J. Chem. Phys.* **2013**, *138*, 114102.
- [27] T. C. Berkelbach, M. S. Hybertsen, D. R. Reichman, *J. Chem. Phys.* **2013**, *138*, 114103.
- [28] C.-H. Yang, C.-P. Hsu, *J. Phys. Chem. Lett.* **2015**, *6*, 1925.
- [29] E. C. Greyson, B. R. Stepp, X. Chen, A. F. Schwerin, I. Paci, M. B. Smith, A. Akdag, J. C. Johnson, A. J. Nozik, J. Michl, M. A. Ratner, *J. Phys. Chem. B* **2010**, *114*, 14223.
- [30] Z. Havlas, J. Michl, *Isr. J. Chem.* **2016**, *56*, 96.
- [31] A. F. Morrison, J. M. Herbert, *J. Phys. Chem. Lett.* **2015**, *6*, 4390.
- [32] A. F. Morrison, Z.-Q. You, J. M. Herbert, *J. Chem. Theory Comput.* **2014**, *10*, 5366.
- [33] M. Wibowo, R. Broer, R. W. A. Havenith, *Comput. Theor. Chem.* **2017**, *1116*, 190.
- [34] A. Zaykov, P. Felkel, E. A. Buchanan, M. J. R. W. A. Havenith, R. K. Kathir, R. Broer, Z. Havlas, J. Michl, *J. Am. Chem. Soc.* **2019**, *141*, 17729.
- [35] T. P. Straatsma, R. Broer, S. Faraji, R. W. A. Havenith, *Ann. Rep. Comput. Chem.* **2018**, *14*, 77.
- [36] T. P. Straatsma, R. Broer, S. Faraji, R. W. A. Havenith, L. E. Aguilar Suarez, R. K. Kathir, M. Wibowo, C. de Graaf, *J. Chem. Phys.* **2020**, *152*, 064111.
- [37] R. K. Kathir, C. de Graaf, R. Broer, R. W. A. Havenith, *J. Chem. Theory Comput.* **2020**, *16*, 2941.
- [38] Z.-Q. You, C.-P. Hsu, G. R. Fleming, *J. Chem. Phys.* **2006**, *124*, 044506.
- [39] Y. Yu Zhang, R. A. Friesner, R. B. Murphy, *J. Chem. Phys.* **1997**, *107*, 450.
- [40] M. F. Guest, I. J. Bush, H. J. J. van Dam, P. Sherwood, J. M. H. Thomas, J. H. van Lenthe, R. W. A. Havenith, J. Kendrick, *Mol. Phys.* **2005**, *103*, 719.

- [41] T. H. Dunning, *J. Chem. Phys.* **1989**, *90*, 1007.
- [42] D. Feller, *J. Comput. Chem.* **1996**, *17*, 1571.
- [43] B. P. Pritchard, D. Altarawy, B. Didier, T. D. Gibbsom, T. L. Windus, A. New Basis, *J. Chem. Inf. Model.* **2019**, *59*, 4814.
- [44] K. L. Schuchardt, B. T. Didier, T. Elsethagen, L. Sun, V. Gurumoorthi, J. Chase, J. Li, T. L. Windus, *J. Chem. Inf. Model.* **2007**, *47*, 1045.
- [45] Verbeek, J.; Langenberg, J. H.; Byrman, C. P.; Dijkstra, F.; Havenith, R. W. A.; Engelberts, J. J.; Zielinski, M.; Rashid, Z.; van Lenthe, J. H. *TURTLE, an ab initio VB/VBSCF program*, Utrecht, The Netherlands, **1988** 2016.
- [46] J. H. van Lenthe, G. G. Balint-Kurti, *Chem. Phys. Lett.* **1980**, *76*, 138.
- [47] J. H. van Lenthe, G. G. Balint-Kurti, *J. Chem. Phys.* **1983**, *78*, 5699.
- [48] G. A. Gallup, J. M. Norbeck, *Chem. Phys. Lett.* **1973**, *21*, 495.
- [49] E. J. Baerends, *ADF2019.03, SCM, Theoretical Chemistry*, Vrije Universiteit, Amsterdam, The Netherlands **2019**.
- [50] G. te Velde, F. M. Bickelhaupt, E. J. Baerends, C. Fonseca Guerra, S. J. A. van Gisbergen, J. G. Snijders, T. Ziegler, *J. Comput. Chem.* **2001**, *22*, 931.
- [51] E. van Lenthe, E. J. Baerends, *J. Comput. Chem.* **2003**, *24*, 1142.
- [52] D. Feller, *J. Chem. Phys.* **1992**, *96*, 6104.
- [53] D. Feller, *J. Chem. Phys.* **1993**, *98*, 7059.
- [54] J. Pipek, P. G. Mezey, *J. Chem. Phys.* **1989**, *90*, 4916.

#### SUPPORTING INFORMATION

Additional supporting information may be found online in the Supporting Information section at the end of this article.

**How to cite this article:** Speelman T, Cunha AV, Kathir RK, Havenith RWA. Electronic couplings for singlet fission: Orbital choice and extrapolation to the complete basis set limit. *J Comput Chem.* 2021;42:326–333. <https://doi.org/10.1002/jcc.26458>